

## Studying Optimum Values of Statistical Model Ingredients for $(\alpha,\gamma)$ and $(\gamma,\alpha)$ Reactions

Halim BÜYÜKUSLU<sup>1\*</sup> 

### Abstract

In order to further develop nuclear models/functions, it is important to test various models and functions included in cross-section calculations based on different reaction types, energy ranges, and masses. In this study, the dependence of nuclear ingredients such as level density,  $\alpha$ -nucleus optical model and  $\gamma$ -ray strength function on the cross-section were illustrated by making systematic calculations in the statistical model window. Reaction cross-section calculations were systematically performed for  $(\alpha,\gamma)$  and  $(\gamma,\alpha)$  reactions, which hold significant importance in astrophysics, on various target nuclei. Theoretical model calculations were compared with experimental data. For each set of experimental and calculated cross sections, the average deviation factor  $\langle F \rangle$  values were determined. The best-fit models and functions for all incoming alpha and gamma energies and for all target nuclei were identified.

**Keywords:**  $(\alpha,\gamma)$  and  $(\gamma,\alpha)$  reactions, alpha optical models, level densities, strength functions, Talys 1.96

## $(\alpha,\gamma)$ ve $(\gamma,\alpha)$ Reaksiyonları için İstatistiksel Model Bileşenlerinin Optimum Değerlerinin İncelenmesi

### Öz

Tesir kesit hesaplamalarında yer alan çeşitli modellerin/fonksiyonların farklı reaksiyon türlerine, enerji aralıklarına ve kütlelere göre test edilmesi, nükleer modellerin daha fazla geliştirilmesi için önemlidir. Bu çalışmada, nükleer seviye yoğunluğu,  $\alpha$ -çekirdek optik modeli ve  $\gamma$ -ray strength fonksiyonu gibi nükleer bileşenlerin tesir kesitine bağımlılığı istatistiksel model penceresinde sistematik hesaplamalar yapılarak gösterildi. Astrofizik reaksiyonlar arasında önemli bir yere sahip olan  $(\alpha,\gamma)$  ve  $(\gamma,\alpha)$  reaksiyonları için, çeşitli hedef çekirdeklerde, reaksiyon tesir kesiti hesaplamaları yapıldı. Teorik model hesaplamaları deneysel verilerle karşılaştırıldı. Deneysel ve hesaplanmış tesir kesitlerin her seti için ortalama sapma faktörü  $\langle F \rangle$  değerleri belirlendi. Tüm alfa ve gama ışını gelme enerjileri ve tüm hedef çekirdekler için en uygun modeller/fonksiyonlar belirlendi.

**Anahtar Kelimeler:**  $(\alpha,\gamma)$  ve  $(\gamma,\alpha)$  reaksiyonları, alfa optik modeli, seviye yoğunluğu, strength fonksiyonları, Talys 1.96

<sup>1</sup> Giresun University, Giresun, Türkiye, [halimbuyukuslu@gmail.com](mailto:halimbuyukuslu@gmail.com)

\*Sorumlu Yazar/Corresponding Author

Geliş/Received: 24.09.2023

Kabul/Accepted: 08.02.2024

Yayın/Published: 15.03.2024

## 1. Introduction

$(\gamma, \alpha)$  reactions are an important member of the astrophysical reactions called the astrophysical p (or  $\gamma$  process) process. This process, also called the  $\gamma$  process, involves about 32 proton-rich nuclides between Se and Hg (Kiss et al., 2014; Rapp et al., 2002). The obtained data from  $(\gamma, \alpha)$  reactions and the inverse  $(\alpha, \gamma)$  reactions are valuable for solving various unknowns in this field. Despite the lack of experimental data, especially on the  $(\gamma, \alpha)$  reaction,  $\alpha$  induced reaction cross-section measurements have been made for many target nuclei by ATOMKI team in recent years (Gyürky et al., 2012; Mohr, 2011, 2013; Mohr et al., 2010, 2020; Szücs et al., 2018; Wilmes et al., 2002). In the mentioned studies, theoretical analyzes of the reactions were also carried out in great detail.

Many nuclear models, functions and their many parameters are taken into account in nuclear cross-section calculations (Büyüksulu, 2019). In order to obtain results that match the experimental data, all these models and parameters must be selected accurately (Kiss et al., 2018; Mohr et al., 2017). The  $(\alpha, \gamma)$  nuclear reactions, which are the subject of astrophysical studies, occur at an incident energy of a few MeV. The compound reaction (CM) mechanism is more dominant in nuclear reactions at medium and low incident energies. Compound-nucleus was successfully formulated with the statistical Hauser–Feshbach (HF) model (Hauser and Feshbach, 1952). HF statistical model calculations, which can give results close to experimental data, are made using the accurate alpha optical model potential and potential parameters. The  $\alpha$ -nucleus optical model potential is the essential ingredient for the calculation of  $\alpha$ -induced reaction cross-sections at low energies. Also input parameters of level densities,  $\gamma$ -ray strength functions are required for nuclear model calculations. Parameters for various nuclear models can be accessed from the RIPL-3 library (Capote et al., 2009) and can also be offered as an option in nuclear reaction codes, as in our study.

In this study, the best values of the essential components of the nuclear statistical model were determined for the  $(\alpha, \gamma)$  and  $(\gamma, \alpha)$  reactions via the TALYS nuclear code. For this purpose, reaction cross-sections were systematically calculated for target nuclei for which experimental data were available. The models/functions to be explained in the next section were compared individually with the default values of the code, and each component was also calculated together for the most optimal value. Comparison of theoretical and experimental results was made using average deviation factor  $\langle F \rangle$ .

## 2. Models and Methods

Nuclear reaction cross sections that can be calculated with nuclear reaction models include the contributions of compound nuclei, pre-equilibrium and direct reaction mechanisms. Experimental

data of the  $(\alpha,\gamma)$  and  $(\gamma,\alpha)$  reactions in the literature consist of data containing nuclear reactions with incident energy that will allow the p process to occur. The effective temperature range for p-nucleus formation is  $1.5 \leq T \leq 3.5$  considering the p-process. (Rauscher et al., 2013). The corresponding Gamow window is located at a few MeV for intermediate-mass nuclei like  $^{64}\text{Zn}$  (Mohr et al., 2017). This energy values varies for different charge and alpha incident energy (Rauscher et al., 2013). It is expected that the compound nucleus contribution to be higher in the mentioned energy range (low and medium energy region). Therefore, the HF statistical model is preferred especially in p reaction process calculations such as theoretical reaction rates. In this study, all HF calculations were carried out with the TALYS 1.96 nuclear reaction code (Koning et al., 2007). The TALYS code is a very successful and widely used tool that can predict nuclear reactions with an incident energy of 200 MeV and a target nuclei mass greater than 12. HF statistical model components are affected by many different models, functions and their parameters. TALYS code allows users to choose these models and the parameters related to the models. Additionally, the code assigns default values for each parameter after installation.

Level Densities (LD), Alfa-nucleus Optical Models ( $\alpha\text{OM}$ ),  $\gamma$ -ray strength functions (STR) are the ingredients that make an essential contribution to the reaction cross-section calculations for  $(\alpha,\gamma)$  and  $(\gamma,\alpha)$  reactions. In addition, at high energies (above approximately 15-20 MeV) it is necessary to take into account the contributions of the pre-equilibrium reaction mechanism (PRE). In this study, PRE-contribution was also added for the  $(\gamma,\alpha)$  reactions due to the high gamma incident energy. The TALYS 1.96 code provides as many options as possible for all these components, ensuring the best calculation result is achieved. The model options offered by the TALYS code for the three components mentioned are listed in Table 1. Details of each alternative model and functions are given in the corresponding reference.

**Table 1.** References and Talys input parameter keywords of the Models/Functions in the study

<i>The Alpha Optical Model Potentials (<math>\alpha\text{OMP}</math>)</i>	<i>Ref.</i>	<i>Talys Keyword</i>
Watanabe folding approach with Koning-Delaroche nucleon potentials	(Koning and Delaroche, 2003; Watanabe, 1958)	alphaomp 1
Alpha potential of McFadden and Satchler	(McFadden and Satchler, 1966)	alphaomp 2
Alpha potential of Demetriou and Goriely, table 1.	(Demetriou et al., 2002)	alphaomp 3
Alpha potential of Demetriou and Goriely, table 2	(Demetriou et al., 2002)	alphaomp 4
Demetriou, Grama and Goriely double folding dispersive potential	(Demetriou et al., 2002)	alphaomp 5
Alpha potential of Avrigeanu et al.	(Avrigeanu et al., 2014)	alphaomp 6*
Alpha potential of Nolte et al.	(Nolte et al., 1987)	alphaomp 7
Alpha potential of Avrigeanu et al.	(Avrigeanu et al., 1994)	alphaomp 8

*Phenomenological and Microscopic Level Density Models (LDM)*

Constant Temperature + Fermi gas model (CTM)	(Gilbert and Cameron, 1965)	ldmodel 1*
Back-shifted Fermi gas Model (BFM)	(Dilg et al., 1973)	ldmodel 2
Generalised Superfluid Model (GSM)	(Ignatyuk et al., 1993)	ldmodel 3
Skyrme-Hartree-Fock-Bogoluybov level densities from numerical tables	(Goriely et al., 2001)	ldmodel 4
Gogny-Hartree-Fock-Bogoluybov level densities from numerical tables	(Goriely et al., 2008)	ldmodel 5
Temperature-dependent Gogny-Hartree-Fock-Bogoluybov level densities from numerical tables	(Hilaire et al., 2012)	ldmodel 6

*E1 gamma-ray strength functions ( $\gamma$  SF)*

Kopecky-Uhl generalized Lorentzian	(Kopecky and Uhl, 1990)	strength 1
Brink-Axel Lorentzian	(Axel, 1962; Brink, 1957)	strength 2*
Hartree-Fock BCS tables	(Goriely and Khan, 2002)	strength 3
Hartree-Fock-Bogoliubov tables	(Goriely et al., 2004)	strength 4
Goriely's hybrid model	(Goriely, 1998)	strength 5
Goriely T-dependent HFB	(Goriely et al., 2004)	strength 6
the temperature-dependent relativistic mean field [32], and	(Daoutidis and Goriely, 2012)	strength 7
the Gogny D1M HFB and quasiparticle random-phase approximation	(Goriely et al., 2018)	strength 8
SMLO	(Goriely and Plujko, 2019)	strength 9

*Pre-equilibrium Reaction Models*

Exciton model: Analytical transition rates with energy-dependent matrix element	(Gruppelaar et al., 1986; Koning and Duijvestijn, 2004)	preeqmode 1
Exciton model: Numerical transition rates with energy-dependent matrix element	(Gruppelaar et al., 1986; Koning and Duijvestijn, 2004)	preeqmode 2*
Exciton model: Numerical transition rates with optical model for collision probability	(Gruppelaar et al., 1986; Koning and Duijvestijn, 2004)	preeqmode 3

\*TALYS default value

Experimental data were compiled from the EXFOR library (Otuka et al., 2014). For the  $(\alpha, \gamma)$  reaction calculations, experimental data from 26 target nuclei with incident energies between 2,7 MeV and 40,7 MeV were used. And for the  $(\gamma, \alpha)$  reaction calculations, experimental data from 7 target nuclei with incident energies between 14 MeV and 27 MeV were used. It can be said that experimental data for the  $(\gamma, \alpha)$  reaction is quite lacking. While experimental data were taken from the EXFOR library, those measured in recent years were preferred. References and incident energy ranges of experimental data taken from the EXFOR library are shown in Table 2.

**Table 2.** Reaction target nucleus, experimental data EXFOR references, projectile incident energy, best fit combinations of model/function sets and <F> for the sets

Target nuclei for ( $\gamma, \alpha$ ) reaction	EXFOR ref. number (SUBENT)	Gamma ray energy range (MeV)	Model/Function Set*	<F>
<sup>51</sup> V	M0894003	15.5-25.1	ldmodel_4/strengthe1_5/preeqmode_2	2.11
<sup>65</sup> Cu	M0894002	15-24.9	ldmodel_6/strengthe1_7/preeqmode_2	7.22
<sup>76</sup> Ge	M0894005	16-25	ldmodel_5/strengthe1_5/preeqmode_3	1.88
<sup>87</sup> Rb	M0273013	15-27	ldmodel_1/strengthe1_3/preeqmode_3	1.73
<sup>93</sup> Nb	M0894004	14-24.9	ldmodel_6/strengthe1_5/preeqmode_2	6.17
<sup>96</sup> Zr	M0894006	16.5-24.9	ldmodel_6/strengthe1_7/preeqmode_3	2.69
<sup>170</sup> Er	M0894007	19.5-24.9	ldmodel_6/strengthe1_1/preeqmode_1	2.36

Target nuclei for ( $\alpha, \gamma$ ) reaction	EXFOR ref. number (SUBENT)	Projectile energy range (MeV)	Parameter/Model Set*	<F>
<sup>34</sup> S	F0824003	2.7-5.8	ldmodel_6/strengthe1_5/alphaomp_3	1.29
<sup>37</sup> Cl	C0669002	2.9-5.2	ldmodel_2/strengthe1_5/alphaomp_5	1.8
<sup>42</sup> Ca	A0310002	3.3-5.6	ldmodel_4/strengthe1_1/alphaomp_3	1.24
<sup>58</sup> Ni	P0072002	12.2-33.1	ldmodel_2/strengthe1_2/alphaomp_5	6,15
<sup>60</sup> Ni	C2181002	5.3-7.3	ldmodel_1/strengthe1_5/alphaomp_3	1.09
<sup>62</sup> Ni	O1534002	4.9-8.9	ldmodel_3/strengthe1_5/alphaomp_6	1.13
<sup>63</sup> Cu	C1050002	5.8-8.6	ldmodel_1/strengthe1_1/alphaomp_7	9.31
<sup>65</sup> Cu	O1761004	5.1-8	ldmodel_3/strengthe1_2/alphaomp_4	1.23
<sup>74</sup> Ge	C2196004	8.9-11.4	ldmodel_6/strengthe1_7/alphaomp_1	1.11
<sup>90</sup> Zr	C2453002	7.8-11.8	ldmodel_1/strengthe1_1/alphaomp_1	4.74
<sup>92</sup> Mo	O1761002	7.6-10.8	ldmodel_4/strengthe1_9/alphaomp_5	1.2
<sup>96</sup> Ru	A0451002	7.3-10.9	ldmodel_1/strengthe1_1/alphaomp_1	21.3
<sup>102</sup> Pd	C2453003	9.2-11.9	ldmodel_1/strengthe1_7/alphaomp_1	2.69
<sup>106</sup> Cd	D4169002	8.4-12.5	ldmodel_6/strengthe1_2/alphaomp_4	1.25
<sup>107</sup> Ag	D4328002	8.8-12.9	ldmodel_3/strengthe1_1/alphaomp_8	1.71
<sup>113</sup> In	C1715002	9-14.1	ldmodel_3/strengthe1_6/alphaomp_1	1.15
<sup>115</sup> In	D4385002	9.1-16.1	ldmodel_3/strengthe1_7/alphaomp_8	1.12
<sup>115</sup> Sn	D0652007	9.5-15.2	ldmodel_3/strengthe1_1/alphaomp_2	36.47
<sup>121</sup> Sb	D4393004	11.4-13.9	ldmodel_3/strengthe1_3/alphaomp_2	1.12
<sup>124</sup> Xe	D4365002	10.4-14.4	ldmodel_4/strengthe1_1/alphaomp_1	9.34
<sup>127</sup> I	C0720007	10.2-40.7	ldmodel_6/strengthe1_5/alphaomp_7	3.59
<sup>130</sup> Ba	D4271002	11.9-16.4	ldmodel_5/strengthe1_8/alphaomp_5	1.27
<sup>136</sup> Xe	P0072003	13.4-38.6	ldmodel_6/strengthe1_1/alphaomp_5	2.38
<sup>139</sup> La	P0029002	14.7-34.6	ldmodel_6/strengthe1_7/alphaomp_4	2.38
<sup>162</sup> Er	D4318002	11.4-16.4	ldmodel_3/strengthe1_8/alphaomp_4	1.2
<sup>168</sup> Yb	O2178003	13.4-15	ldmodel_3/strengthe1_2/alphaomp_2	1.2

\*Models/Functions were given with their Talys input keywords

Statistical analysis methods such as average deviation factor <F> are used to determine the quality of the comparison of experimental data and theoretical calculations. In order to determine the best model/function set, <F> value was calculated for both reactions for all target nucleus and each incident energy. An average deviation factor is defined by

$$\langle F \rangle = 10^{\sqrt{s}} \quad s = \frac{1}{N} \sum_{i=1}^N (\log \sigma_{exp} - \log \sigma_{theo})^2 \quad (1)$$

### 3. Results and Discussion

Calculations to obtain the optimum function and model set are divided into two parts. The first part of the calculations is the calculation of all combinations of the  $\alpha$ OM, LD and STR models that the TALYS code gives as options. For the  $(\alpha,\gamma)$  reaction, 432 combinations (8 for  $\alpha$ OM, 6 for LD and 9 for STR) were calculated for each 26 target nuclei. On the other hand, for  $(\gamma,\alpha)$  reaction, 162 combinations (3 for PRE, 6 for LD and 9 for STR) were calculated for each 7 target nuclei. The model set in which the lowest  $\langle F \rangle$  value is achieved, in other words, the cross-section values that overlap with the experimental data are obtained, is given in Table 2 for each target nuclei.

In the second part of the calculations, while all other models and functions were at default settings, the options for  $\alpha$ OM, LD, STR and PRE were calculated separately. In this case, models that gives best agreement with experimental data were identified among 8  $\alpha$ OM, 6 LD and 9 STR models for the  $(\alpha,\gamma)$  reaction and among 2 PRE, 6 LD and 9 STR for the  $(\gamma,\alpha)$  reactions. For this second case, a separate categorization was made according to the target nucleus mass and its incident energy. Their graphics are given in Figure 1-3. The model numbers that give the most compatible calculations with the experimental cross-section according to  $\langle F \rangle$  values are shown with histogram graphics.

#### 3.1. $(\alpha,\gamma)$ reaction calculations

Calculations were carried out with a combination of  $\alpha$ OM, LD, STR options to reach the best-fit results. Best-fit combinations and calculated average deviation factors  $\langle F \rangle$  were listed in Table 2 for 26 target nuclei.  $\langle F \rangle$  factor varies between 1.09-36.47. Best-fit calculation is obtained from a ldmodel\_1, strength1\_5, alphaomp\_3 for the  $^{60}\text{Ni}$  nucleus.

The results obtained for the  $(\alpha,\gamma)$  reactions in Fig. 1 are divided into two groups as target nucleus mass number less than 74 (8 nuclei) and larger (18 nuclei). It seems that aomp\_2 and aomp\_4, among the alpha optical model versions used for  $A > 74$  nuclei, are more compatible. Among the  $\gamma$ -ray strength functions, the first and second (strength\_1 and strength\_2) are clearly the best strength functions, while ldmodel\_3 is the most successful model for LD. For  $A < 74$  nuclei, there is no model that stands out from the alpha optical models and LD models, but it can be said that the 1st and 7th functions (strength\_1 and strength\_7) are successful among the  $\gamma$ -ray strength functions.

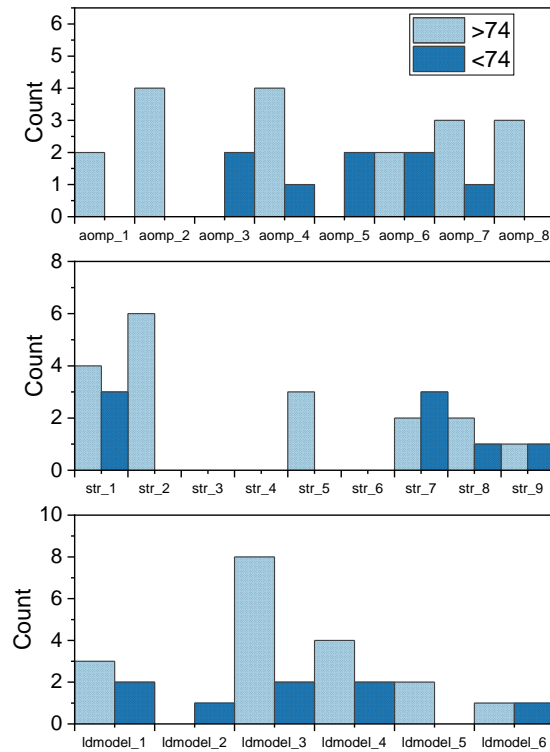


**Figure 1.** Histogram showing the best fit number of models for the  $(\alpha, \gamma)$  reaction on  $<74$  and  $>74$  target mass number range

A comparison of the models used at different alpha energies for the  $(\alpha, \gamma)$  reaction is given in Fig. 2. In Fig. 2 (a), calculations were made for 26 target nuclei up to incident energies specified in the corresponding reference. We cannot say that the alpha optical models used give very different values from each other. Only 4th model (aomp\_4) seems to make slightly more optimal calculations. Among the LD models, third and 4th models have a clear superiority in a wider energy range, while strength\_1, strength\_2 and strength\_7 are successful among the  $\gamma$ -ray strength functions. In the 14-15 MeV energy region (Fig. 2 (b)), all of them are similar except the 9th (aomp\_9) alpha optical models. It can be said that 3rd and 5th models in LD and all functions except the 5th and 6th functions in  $\gamma$ -ray strength functions are successful. The histogram graph of the calculations made for the alpha incident energy below 10 MeV in the reaction on 17 target nuclei is given in Fig.2 (c). It is seen that all alpha optical models, except the 1st and 9th models, give similar successful calculation results. 1st, 3rd and 4th LD models were appeared in more successful calculations. Finally, for  $\gamma$ -ray strength functions, the 1st, 7th and 8th functions are more compatible with the experimental data.

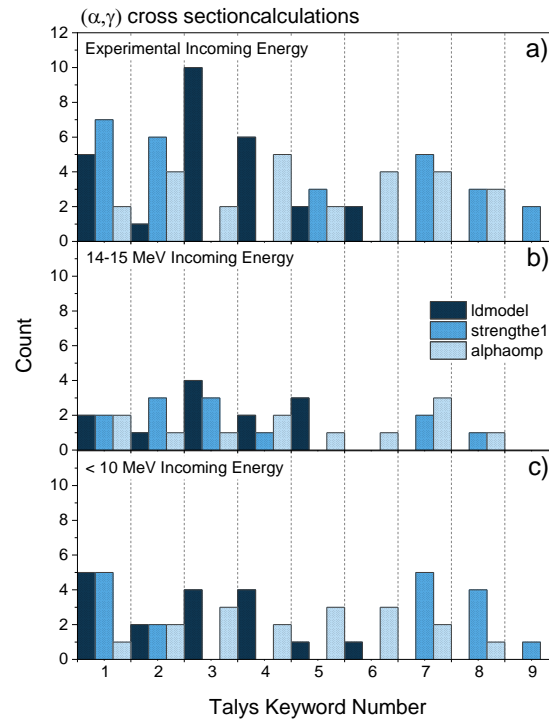


**Figure 2.** Histogram showing the best fit number of models for the  $(\alpha,\gamma)$  reaction a) up to experimental incoming energy b) at the incoming energy range 14-15 MeV c) below the 10 MeV incoming energy. Horizontal numbers correspond to the models' keywords in the Talys code.

### 3.2. $(\gamma,\alpha)$ reaction calculations

Best-fit  $(\gamma,\alpha)$  reaction cross-sections for 7 target nuclei were calculated via combinations of Level density,  $\gamma$ -ray strength functions and pre-equilibrium model options. Due to the high incoming energy value, models of the pre-equilibrium nuclear reaction mechanism were also included in this part of the calculations. Fit combinations and calculated average deviation factors  $\langle F \rangle$  were listed in Table 2.  $\langle F \rangle$  factor has its lowest value at 1.73 and its highest value at 7.22. Best-fit calculation is obtained from a ldmodel\_1, strengthe1\_3, preeqmode\_3 for the  $^{87}\text{Rb}$  nucleus.

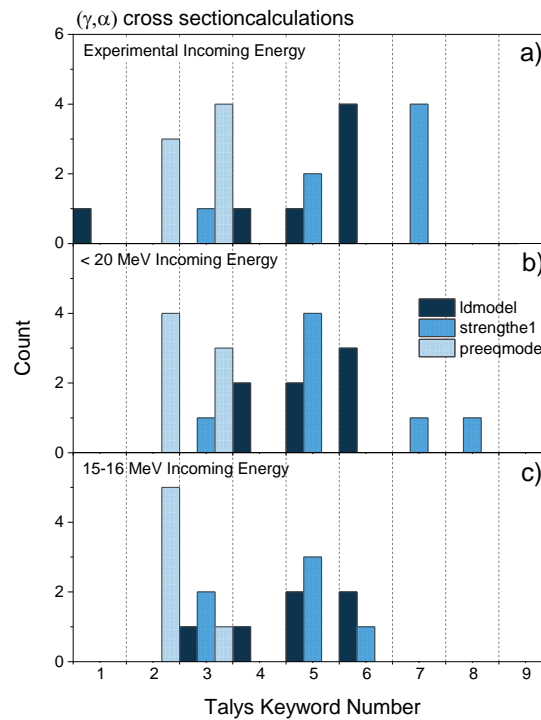


**Figure 3.** Histogram showing the best fit number of models for the  $(\gamma,\alpha)$  reaction a) up to experimental incoming energy b) below the 20 MeV incoming energy c) at the incoming energy range 15-16 MeV. Horizontal numbers correspond to the models' keywords in the Talys code.

In Fig. 3, a comparison of the models used at different gamma energies for the  $(\gamma,\alpha)$  reaction is given. In Fig. 3 (a), calculations were made for 7 target nuclei up to incident energies specified in the corresponding reference. Although pre-equilibrium model preeqmode\_1 was included in the calculations, it did not make it to the success list. Among the pre-equilibrium models used, preeqmode\_3 had the smallest  $\langle F \rangle$  value, only one more value than preeqmode\_2. ldmodel\_6 from LD models and strength\_7 from  $\gamma$ -ray strength functions are clearly more successful. In Fig3 (b), which shows the incident energy region below 20 MeV, 2th model from pre-equilibrium models and the 6th model among the LD models are as successful as the previous. Among the  $\gamma$ -ray strength functions, strength\_5 clearly achieved the highest number of successes. Finally, in the calculations made for 6 nuclei in the 15-16 MeV energy region (Fig.3 (c)), preeqmode\_2 is by far superior to the pre-equilibrium models. All LD models have achieved success rates close to each other. Among the  $\gamma$ -ray strength functions, strength\_5 achieved more successful calculations.

#### 4. Conclusions

Within the framework of the statistical model, various models/functions that affect the reaction cross-section value were tested for  $(\alpha,\gamma)$  and  $(\gamma,\alpha)$  reactions. For the  $(\alpha,\gamma)$  reactions, 26 experimental data were considered, while for the  $(\gamma,\alpha)$  reaction, fewer experimental data (only 6 target nuclei) were

found. The cross-section calculations were made using the options  $\alpha$ +nucleus optical model (for  $(\alpha,\gamma)$  reactions), level density,  $\gamma$ -ray strength function and pre-equilibrium model (for  $(\gamma,\alpha)$  reaction), both together and separately. The best model and model set combinations were determined.

In the calculations made by taking the models into account together, the Temperature-dependent Gogny-Hartree-Fock-Bogoluybov level density model appeared more frequently among the best 162 combinations for the  $(\gamma,\alpha)$  reactions. The pre-equilibrium model and  $\gamma$ -ray strength function options showed a more homogeneous distribution. among the level densities, the Generalized Superfluid Model (GSM) and among the  $\gamma$ -ray strength functions, the Kopecky-Uhl generalized Lorentzian function were more in the best combination for the  $(\alpha,\gamma)$  reactions.

Individual model calculations differed within each mass range and energy range. This result is due to the energy and mass ranges for which the models are valid. For example, while the number of most successful models is approximately equal in the  $<74$  region, the Brink-Axel Lorentzian function and the Generalized Superfluid Model (GSM) model give the best results in the  $>74$  region. In energy ranges, the Generalized Superfluid Model (GSM) model was approximately the best at all energies for the  $(\alpha,\gamma)$  reactions, while Temperature-dependent Gogny-Hartree-Fock-Bogoluybov level densities got the best results for the  $(\gamma,\alpha)$  reaction. In this part of the calculations, the first pre-equilibrium model (Exciton model: Numerical transition rates with optical model for collision probability) could not be found successful for both reaction types.

### Statement of Research and Publication Ethics

The author declares that this study complies with Research and Publication Ethics.

### References

- Avriganu, V., Avriganu, M., and Mănăilescu, C. (2014). Further explorations of the  $\alpha$ -particle optical model potential at low energies for the mass range  $A \approx 45 - 209$ . *Physical Review C*, 90(4), 044612.
- Avriganu, V., Hodgson, P. E., and Avriganu, M. (1994). Global optical potentials for emitted alpha particles. *Physical Review C*, 49(4), 2136–2141.
- Axel, P. (1962). Electric Dipole Ground-State Transition Width Strength Function and 7-Mev Photon Interactions. *Physical Review*, 126(2), 671–683.
- Brink, D. M. (1957). Individual particle and collective aspects of the nuclear photoeffect. *Nuclear Physics*, 4(C), 215–220.
- Büyüksulu, H. (2019). Parametrization study for the estimation of light particles (p, d,  $^3\text{He}$ ,  $\alpha$ ) induced total reaction cross sections of target mass greater than 9 within the energy range of 10–200 MeV. *Radiation Physics and Chemistry*, 165, 108431.
- Capote, R., Herman, M., Obložinský, P., Young, P. G., Goriely, S., Belgya, T., Ignatyuk, A. V., Koning, A. J., Hilaire, S., Plujko, V. A., Avriganu, M., Bersillon, O., Chadwick, M. B., Fukahori, T., Ge, Z., Han, Y., Kailas, S., Kopecky, J., Maslov, V. M., ... Talou, P. (2009). RIPL – Reference Input Parameter Library

- for Calculation of Nuclear Reactions and Nuclear Data Evaluations. *Nuclear Data Sheets*, 110(12), 3107–3214.
- Daoutidis, I., and Goriely, S. (2012). Large-scale continuum random-phase approximation predictions of dipole strength for astrophysical applications. *Physical Review C*, 86(3), 034328.
- Demetriou, P., Grama, C., and Goriely, S. (2002). Improved global  $\alpha$ -optical model potentials at low energies. *Nuclear Physics A*, 707(1–2), 253–276.
- Dilg, W., Schantl, W., Vonach, H., and Uhl, M. (1973). Level density parameters for the back-shifted fermi gas model in the mass range  $40 < A < 250$ . *Nuclear Physics A*, 217(2), 269–298.
- Gilbert, A., and Cameron, A. G. W. (1965). A composite nuclear-level density formula with shell corrections. *Canadian Journal of Physics*, 43(8), 1446–1496.
- Goriely, S. (1998). Radiative neutron captures by neutron-rich nuclei and the r-process nucleosynthesis. *Physics Letters B*, 436(1–2), 10–18.
- Goriely, S., Hilaire, S., and Koning, A. J. (2008). Improved microscopic nuclear level densities within the Hartree-Fock-Bogoliubov plus combinatorial method. *Physical Review C*, 78(6), 064307.
- Goriely, S., Hilaire, S., Péru, S., and Sieja, K. (2018). Gogny-HFB+QRPA dipole strength function and its application to radiative nucleon capture cross section. *Physical Review C*, 98(1), 014327.
- Goriely, S., and Khan, E. (2002). Large-scale QRPA calculation of E1-strength and its impact on the neutron capture cross section. *Nuclear Physics A*, 706(1–2), 217–232.
- Goriely, S., Khan, E., and Samyn, M. (2004). Microscopic HFB + QRPA predictions of dipole strength for astrophysics applications. *Nuclear Physics A*, 739(3–4), 331–352.
- Goriely, S., and Plujko, V. (2019). Simple empirical E1 and M1 strength functions for practical applications. *Physical Review C*, 99(1), 014303.
- Goriely, S., Tondeur, F., and Pearson, J. M. (2001). A hartree–fock nuclear mass table. *Atomic Data and Nuclear Data Tables*, 77(2), 311–381.
- Gruppelaar, H., Nagel, P., and Hodgson, P. E. (1986). Pre-equilibrium processes in nuclear reaction theory. *The state-of-the-art and beyond*. 9:7.
- Gyürky, Gy., Mohr, P., Fülöp, Zs., Halász, Z., Kiss, G. G., Szücs, T., and Somorjai, E. (2012). Relation between total cross sections from elastic scattering and  $\alpha$ -induced reactions: The example of  $^{64}\text{Zn}$ . *Physical Review C*, 86(4), 041601.
- Hauser, W., and Feshbach, H. (1952). The Inelastic Scattering of Neutrons. *Physical Review*, 87(2), 366–373.
- Hilaire, S., Girod, M., Goriely, S., and Koning, A. J. (2012). Temperature-dependent combinatorial level densities with the DIM Gogny force. *Physical Review C*, 86(6), 064317.
- Ignatyuk, A. V., Weil, J. L., Raman, S., and Kahane, S. (1993). Density of discrete levels in  $\text{Sn}116$ . *Physical Review C*, 47(4), 1504–1513.
- Kiss, G. G., Szücs, T., Mohr, P., Török, Zs., Huszánk, R., Gyürky, Gy., and Fülöp, Zs. (2018).  $\alpha$ -induced reactions on  $\text{In}115$ : Cross section measurements and statistical model analysis. *Physical Review C*, 97(5), 055803.
- Kiss, G. G., Szücs, T., Rauscher, T., Török, Z., Fülöp, Z., Gyürky, G., Halász, Z., and Somorjai, E. (2014). Alpha induced reaction cross section measurements on  $^{162}\text{Er}$  for the astrophysical  $\gamma$  process. *Physics Letters B*, 735, 40–44.
- Koning, A. J., and Delaroche, J. P. (2003). Local and global nucleon optical models from 1 keV to 200 MeV. *Nuclear Physics A*, 713(3–4), 231–310.
- Koning, A. J., and Duijvestijn, M. C. (2004). A global pre-equilibrium analysis from 7 to 200 MeV based on the optical model potential. *Nuclear Physics A*, 744, 15–76.
- Koning, A. J., Hilaire, S., and Duijvestijn, M. C. (2007, May 21). TALYS-1.0. *ND2007*.
- Kopecky, J., and Uhl, M. (1990). Test of gamma-ray strength functions in nuclear reaction model calculations. *Physical Review C*, 41(5), 1941–1955.
- McFadden, L., and Satchler, G. R. (1966). Optical-model analysis of the scattering of 24.7 MeV alpha particles. *Nuclear Physics*, 84(1), 177–200.
- Mohr, P. (2011). Total reaction cross sections from  $^{141}\text{Pr}$  ( $\alpha, \alpha$ )  $^{141}\text{Pr}$  elastic scattering and  $\alpha$ -induced reaction cross sections at low energies. *Physical Review C*, 84(5), 055803.
- Mohr, P. (2013). Total reaction cross section  $\sigma_{\text{reac}}$  of  $\alpha$ -induced reactions from elastic scattering: The example  $^{140}\text{Ce}$  ( $\alpha, \alpha$ )  $^{140}\text{Ce}$ . *Physical Review C*, 87(3), 035802.
- Mohr, P., Fülöp, Zs., Gyürky, Gy., Kiss, G. G., and Szücs, T. (2020). Successful Prediction of Total  $\alpha$ -Induced Reaction Cross Sections at Astrophysically Relevant Sub-Coulomb Energies Using a Novel Approach. *Physical Review Letters*, 124(25), 252701.

- Mohr, P., Galaviz, D., Fülöp, Zs., Gyürky, Gy., Kiss, G. G., and Somorjai, E. (2010). Total reaction cross sections from elastic  $\alpha$ -nucleus scattering angular distributions around the Coulomb barrier. *Physical Review C*, 82(4), 047601.
- Mohr, P., Gyürky, Gy., and Fülöp, Zs. (2017). Statistical model analysis of  $\alpha$ -induced reaction cross sections of Zn64 at low energies. *Physical Review C*, 95(1), 015807.
- Nolte, M., Machner, H., and Bojowald, J. (1987). Global optical potential for  $\alpha$  particles with energies above 80 MeV. *Physical Review C*, 36(4), 1312–1316.
- Otuka, N., Dupont, E., Semkova, V., Pritychenko, B., Blokhin, A. I., Aikawa, M., Babykina, S., Bossant, M., Chen, G., Dunaeva, S., Forrest, R. A., Fukahori, T., Furutachi, N., Ganesan, S., Ge, Z., Gritzay, O. O., Herman, M., Hlavač, S., Kato, K., ... Zhuang, Y. (2014). Towards a More Complete and Accurate Experimental Nuclear Reaction Data Library (EXFOR): International Collaboration Between Nuclear Reaction Data Centres (NRDC). *Nuclear Data Sheets*, 120, 272–276.
- Rapp, W., Heil, M., Hentschel, D., Käppeler, F., Reifarh, R., Brede, H. J., Klein, H., and Rauscher, T. (2002).  $\alpha$ - and neutron-induced reactions on ruthenium isotopes. *Physical Review C*, 66(1), 015803.
- Rauscher, T., Dauphas, N., Dillmann, I., Fröhlich, C., Fülöp, Z., and Gyürky, G. (2013). Constraining the astrophysical origin of the p-nuclei through nuclear physics and meteoritic data. *Reports on Progress in Physics*, 76(6), 066201.
- Szücs, T., Kiss, G. G., Gyürky, G., Halász, Z., Fülöp, Z., and Rauscher, T. (2018). Cross section of  $\alpha$ -induced reactions on iridium isotopes obtained from thick target yield measurement for the astrophysical  $\gamma$  process. *Physics Letters B*, 776, 396–401.
- Watanabe, S. (1958). High energy scattering of deuterons by complex nuclei. *Nuclear Physics*, 8(C), 484–492.
- Wilmes, S., Wilmes, V., Staudt, G., Mohr, P., and Hammer, J. W. (2002). The  $^{15}\text{N}(\alpha,\gamma)^{19}\text{F}$  reaction and nucleosynthesis of  $^{19}\text{F}$ . *Physical Review C*, 66(6), 065802.